

A Hybrid Evolutionary Algorithm and its Application to Parameter Identification of Rolling Elements Bearings

Eric Yonghan Kim¹, Bo-Suk Yang² and Andy Chit Chow Tan¹

¹Queensland University of Technology, ²Pukyong National University
¹Australia, ²South Korea

1. Introduction

Genetic algorithms (GAs) are powerful stochastic search techniques and are the most widely known types of evolutionary algorithms (EAs). This method performs a search by evolving a population of candidate solutions through the use of non-deterministic operators and by improving incrementally the individuals forming the population by mechanisms inspired from those of genetics (e.g. crossover and mutation). They are known to offer significant advantages over traditional methods by using simultaneously several search principles and heuristics, of which the most important ones are: population-wide search, continuous balance between exploitation (convergence) and exploration (maintained diversity) and the principle of building-block combination. However, GA can suffer from excessively slow convergence before providing an accurate solution. This is because of its fundamental requirement of using minimal prior knowledge without exploiting local information. Since the introduction of global search algorithms in engineering applications, many modified versions of GA have been reported to reduce the searching time and to raise the global search capability. Many researchers have proposed improved versions of GA which GA operator works adaptively (Wu et al., 1999; He et al., 2001; Fung et al., 2002). A local search or meta-heuristic algorithm has been incorporated into GA to improve the algorithm (Renders & Flasse, 1996; Berger et al., 1999; Lee et al., 2001; Hsiao et al., 2001; Hagenman et al., 2003; Jiang et al., 2003). The combined GA-SA algorithm has been introduced to improve the efficiency of the global search (Roach & Nagi, 1996; Yu et al., 2000; Ong et al., 2002; Liu et al., 2002; Ponnambalam et al., 2003).

In the first half of this chapter, a new hybrid evolutionary algorithm known as clustering-based hybrid evolutionary algorithm (CHEA) is introduced (Kim et al., 2006). This algorithm utilizes the GA's grouping property which involves gathering a number of individuals around the global candidate according to the generation. Clustering of individuals using artificial neural network (ANN) is incorporated into the GA to evaluate the stage of maturity of genetic evolution and to deal with statistical data of each cluster. After clustering, a local search is carried out for each cluster to accelerate the convergence process and to judge the convexity of each cluster. Finally, an efficient random search is adapted for searching the potential global candidate which may be missed in GA and local search. The efficiency of the proposed algorithm is then verified by applying it to three well-

known benchmark functions namely banana function, multi-modal function and Rastrigin function.

The dynamic behavior of a rotating shaft is significantly influenced by the stiffness and damping characteristics of the bearings. The precise values of stiffness and damping coefficients are difficult to predict. In the past decade, many works have dealt with identification of bearing coefficients using impulse or synchronous/non-synchronous excitation techniques (Burrows & Stanway, 1977; Kraus et al., 1987), and using mathematical formulations using an out-of-unbalance response (Lee & Hong, 1988; Chen & Lee, 1995, 1997). Other researches used the least square method as an optimizer to minimize the error between the measured unbalance response and the estimated one after they have formulated the minimization problem (Edwards et al., 2000; Reddy et al., 2002 and Tiwari et al., 2002). Least square method with sensitivity-based approach is a very effective algorithm that can be used for parameter identification of machinery characteristics. However, the application of least square optimizer cannot guarantee a global minimum, which means the identified parameters may not be the optimum ones for the real rotor-bearing systems which are often influenced by noises or non-linear effects.

Recently, global optimization schemes such as GA and simulated annealing (SA) (Kirpatrick et al., 1983) have been used in the area of parameter identification. These schemes do not involve gradient information and mathematical formulation but require only forward analysis procedure. Unfortunately identification approach based on global optimization algorithms is a highly time consuming task because it is based on the iterative strategy which updates unknown parameters systematically using an analytical output. Therefore, a fast and more efficient search algorithm is required for parameter identification in line with the rapid progress of computer technology.

In the latter half of this chapter, we introduce a method of using a hybrid evolutionary algorithm for parameter identification of ball bearings (Kim et al., 2007). The identification method utilises the hybrid evolutionary algorithm. The capability of the technique is verified using a numerical example and a series of experimentation on a tests. The results reveal that the proposed method can identify not only unknown bearing parameters but also unbalance information of disks. In contrast to other traditional identification techniques, the method can be applied with simple formulation of an optimisation problem using the existing dynamic analysis procedure without any complex mathematical approach.

2. Clustering-based hybrid evolutionary algorithm (CHEA)

The CHEA is a hybrid GA which is combined with neural-network, local search and random search. The flowchart of CHEA process is shown in Fig. 1. The first task is *GA-clustering*, in which GA is combined with the clustering process by using neural network. In this task, all individuals after each generation of GA are classified into several clusters until all individuals are well classified. After *GA-clustering*, the local search (LS) is carried out for each cluster with their best individuals. If all final points of the local search converged close to one point, this point implies a global candidate. This means that, graphically, the objective function is a kind of convex, which has only one global/local minimum in the search space. If all final points do not converged to one point, the objective function is considered to be a multi-modal function, which has many local minima. In this case,

additional local searches are carried out which starts at several random points within each group to determine whether each cluster has only one local minimum or not. Similarly, considering one cluster, if the final points by the local search are nearly the same point, this cluster has one local minimum, which implies the objective function is a convex for the region of this cluster. Otherwise the clusters have many local minima in their regions. In this case, GA is run again with reduced bounds as those of each cluster. The classification and the local search procedure are executed until each cluster has only one local minimum. Finally, an efficient random search is adopted for extra-searching to find the potential global candidate which may be missed in GA and local search.

Adaptive resonance theory-Kohonen neural network (ART-KNN) developed by (Yang et al., 2004) is incorporated for clustering of individuals after each generation in GA. Sequential quadratic programming (SQP) is adopted for the task of local search in this algorithm.

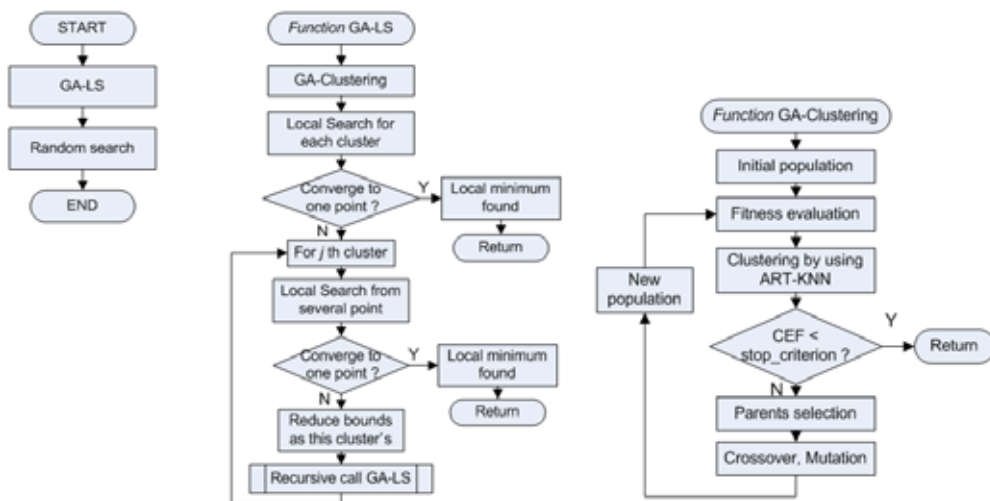


Fig. 1. Flowchart of CHEA

2.1 GA-clustering task

GA improves the genes of individuals based on evolutionary operation. Geometrically, the evolution of GA is that increasing individuals are gathered together around the global or local minimum with respect to the increase of generation as shown in Fig. 2. Generally GA is not efficient for improving the precision of best individuals to global minimum after gathering around the global minimum. However, the ability to gather individuals to a global or local minimum in the first several generations is excellent. Therefore, the proposed hybrid algorithm intends to use the merit of GA and to prevent inefficient calculations after the individuals have gathered around the global or local minimum.

If the objective function is a multi-modal function which has more than two local minimums, clustering or classification of individuals are necessary to divide them into several clusters as shown in Fig. 2(b) and requires a stop criterion for GA.. The clustering evaluation function (CEF) is introduced to evaluate the stage of maturity of individuals in each generation. CEF is defined by eq (1) using statistical data of each classified cluster:

$$CEF = \sum_{j=1}^M \frac{\delta_j \gamma_j}{M \alpha_j \beta_j} \tag{1}$$

$$\delta_j = \sum_{i=1}^{N_j} \|\mathbf{v}_{ij} - \mathbf{v}_{0j}\|^2, \quad \alpha_j = \left(\frac{N_j}{\sum N_j} \right)^{w_g}, \quad \beta_j = \left(\|\mathbf{v}_{0j} - \mathbf{v}_{0all}\|_{\min} \right)^{w_m}, \quad \gamma_j = (1-\rho)^{w_r}$$

where, \mathbf{v}_{ij} denotes the i th vector for the j th cluster and \mathbf{v}_{0j} is the center of the j th cluster. w_g, w_m, w_r are weight factors for cluster, distance of each group and similarity by ART-KNN, respectively. $\| \cdot \|$ denotes Euclidian distance between two vectors. M denotes the number of cluster and N_j is the number of individual for the j th cluster.

In this study, well matured is defined when the average distance from the mid point of each cluster approaches a small value and the average distance among mid points approaches a large value. CEF value for *stop criterion* is very important because it is directly related to the efficiency of the search algorithm. GA stopped with a too high CEF implies that the GA evolution is not matured yet and individuals may be classified into too many clusters. On the contrast, with a too small CEF , most individuals will migrate to only one cluster which contains the best individual. This may lead to lose of useful information about local minimum. Furthermore, if the number of individuals is not sufficient to find all the local minima, most individuals will move to a local minimum. In our study with trying many kind of test functions, the best *stop criterion* is selected as 0.2.

As shown in the flowchart of GA-clustering task in Fig. 1, ART-KNN algorithm was adapted as the traditional GA procedure to classify individuals into several clusters after the evaluation of fitness. After clustering, it is judged whether all individuals are well matured by using the CEF . If the CEF is smaller than the *stop criterion*, subroutine *GA-clustering* is terminated and returns to the final individuals and provides cluster information to the main program. Otherwise, the general procedure of GA, such as selection, crossover and mutation, is preceded again.

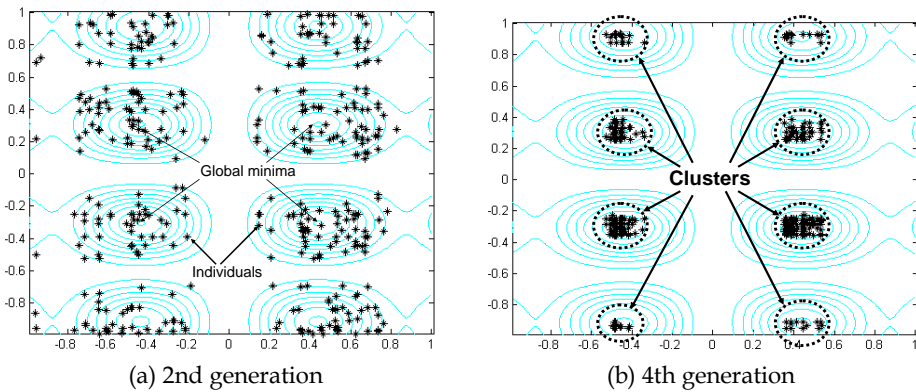


Fig. 2. Distribution of individuals according to generations

2.2 ART-KNN algorithm

The adaptive resonance theory (ART) network (Carpenter & Grossberg, 1988) is a neural network that self-organizes stable recognition codes in real time in response to arbitrary

sequences of input patterns. It is also a vector classifier based on mathematical model for the description of fundamental behavioral functions of the biological brain such as the learning, parallel and distributed information storage, short and long-term memory and pattern recognition. The Kohonen neural network (KNN) (Kohonen, 1995) is also called self-organizing feature map network (SOFM). It defines a feed forward two-layer neural network that implements a characteristic non-linear projection from the high dimensional space of sensory or other input signals onto a low-dimensional array of neurons.

Recently, Yang et al. proposed a new algorithm using the adaptive resonance theory-Kohonen neural network (ART-KNN) (Yang et al., 2004), which does not affect the initial training and can adapt with additional training data. The structure of ART-KNN is shown in Fig. 3. It is similar to ART's but excluding the adaptive filter. ART-KNN is formed by two major subsystems: the attentional subsystem and the orienting subsystem. There are two interconnected layers, discernment layer and comparison layer, which are fully connected with both bottom-up and top-down processes and comprise of the attentional subsystem. The application of a single input vector leads to several patterns of neural activity in both layers. The activity in discernment nodes reinforces the activity in comparison nodes due to top-down connections. The interchange of bottom-up and top-down information leads to a resonance in neural activity. As a result, critical features comparison is reinforced with those having the greatest activity. The orienting subsystem is responsible for generating a reset signal to discernment when the bottom-up input pattern and top-down template pattern do not match during comparison process according to a similarity law. In other words, once it has detected that the input pattern is novel, the orienting subsystem must prevent the previously organized category neurons in discernment from learning this pattern (via a reset signal). Otherwise, the category will become increasingly non-specific. When a mismatch is detected, the network adapts its structure by immediately storing the novelty with additional weights. The similarity criterion is set by the value of the similarity parameter. A high value of the similarity parameter means than only a slight mismatch will be tolerated before a reset signal is emitted. On the other hand, a small value means that large mismatches will be tolerated. After the resonance check, if a pattern match is detected according to the similarity parameter, the network changes the weights of the winning node.

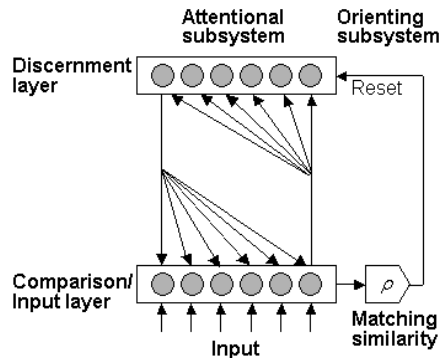


Fig. 3. Structure of ART-KNN

2.3 Clustering by ART-KNN

In the ART-KNN, the determination of a limiting value of similarity (ρ) is important in the optimization problem because the classification result is dependent on ρ . *CEF* detailed in the previous section is used to evaluate the superiority of the classified results based on average distance from mid point of each cluster and the variance of each cluster.

ART-KNN is modified and incorporated into GA procedure for the clustering process according to following sequence:

Step 1: Normalize every individuals of GA from 0 ~ 1.0.

Step 2: Change similarity ρ from 0.4~1.0.

- Classify into clusters using ART-KNN for each ρ .
- Calculate the *CEF* for each ρ .

Step 3: Choose clustering results which correspond to minimum *CEF*.

2.4 Sequential quadratic programming (SQP)

SQP method represents the state of the art in nonlinear programming methods. Schittkowski (Schittkowski, 1985) has implemented and tested a version that outperforms every other tested methods in terms of efficiency, accuracy and percentage of successful solutions over a large number of test problems. Based on the work of Powell (Powell, 1978), the method allows it to closely mimic Newton's method for constrained optimization similar to an unconstrained optimization. At each major iteration, an approximation is made of the Hessian of the Lagrangian function using a quasi-Newton updating method. This is then used to generate a QP sub-problem whose solution is used to form a search direction for a line search procedure. An overview of SQP can be seen in Fletcher (Fletcher, 1980). The general method is not listed here, but MATLAB program provides a full implementation together with the SQP algorithm.

2.5 Efficient random search

The last procedure of CHEA is a complementary random search to find a global minimum candidate, which may be missed in GA and LS procedure. Considering the valley of global minimum is highly narrow and deep as shown in Fig. 4, general stochastic global search algorithms, such as GA and SA, often fail to find the global minimum. This is because not only we use limited number of trials to find the global minimum but heuristics reduce the searching area toward the global candidate which has a relatively wide valley. The mutation operator in GA gives a part of this random search by changing the genes randomly, but it doesn't use previous search history at all. Therefore, this paper proposes an efficient random search method, which uses all previous search points. It works by generating a new search point as far as possible from all previous search points. In the stochastic viewpoint, this random search increases the probability of finding the global minimum.

The steps of the proposed efficient random search are as follows:

Step 1: Generate 5 search points randomly.

Step 2: Calculate Euclidean distance of the nearest point among previous search points.

Step 3: Select one point which has the largest Euclidean distance.

Step 4: Calculate fitness from the objective function.

If the calculated fitness is smaller than the best local minimums from GA-LS,

Step 5: Apply local search using the SQP.

Step 6: Else, go to step 1, repeat the above procedure until the maximum number of iterations is reached.

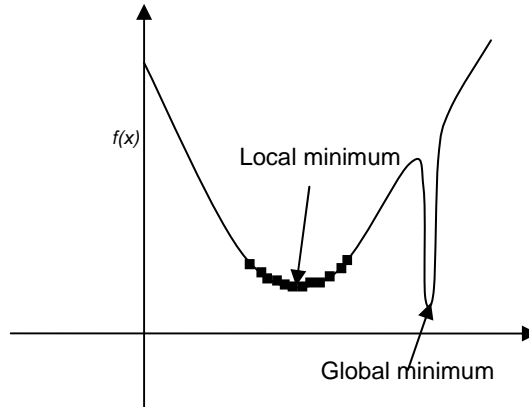


Fig. 4. An objective function which has narrow and deep global minimum

3. Application to test functions

The new optimization algorithm was tested by using several benchmark functions to evaluate its capability and to compare it with other algorithms. Many types of test functions have been used to this subject, however in this study, the three well-known test functions were used to evaluate the algorithm.

- Test function 1: Banana function which has one global minimum and converges slowly to the global minimum.
- Test function 2: Multi-modal function which has several global minima and several local minima
- Test function 3: Rastrigin function which contains one global minimum and many local minima

$$f_1(x_1, x_2) = 100(x_1 - x_2)^2 + (1 - x_1)^2, \quad (-2.0 \leq x_1, x_2 \leq 2.0) \quad (2)$$

$$f_2(x_1, x_2) = (\cos 2\pi x_1 + \cos 2.5\pi x_1 - 2.1) \times (2.1 - \cos 3\pi x_2 - \cos 3.5\pi x_2) \quad (-1.0 \leq x_1, x_2 \leq 1.0) \quad (3)$$

$$f_3(x_1, x_2) = 2 \times 10 + \sum_{i=1}^2 \{x_i^2 - 10 \cos(2\pi i)\} \quad (-5.0 \leq x_1, x_2 \leq 5.0) \quad (4)$$

Test function 1, known as a Banana function, has the shape shown in Fig. 5 (a). In general, the convergence speed of an evolution program for this function is very slow and the accuracy of the searched solution is low as well. The objective of this example is to find the variable \mathbf{x} , which minimizes the objective function. This function has only one optimum solution ($x_1 = 1.0, x_2 = 1.0$) at $f(\mathbf{x}) = 0$. It is difficult to find the optimum solution because of a valley phenomenon. In general, an objective function which has several global minima

and/or local optimum points is called the multi-modal function as shown in Fig. 5 (b). The objective of this test function is to maximize the objective function. This function has four local minima of $f(\mathbf{x})=14.333087$ and four global minima of $f(\mathbf{x})=16.09172$. The Rastrigin function defined in eq. (4) is often used to evaluate the global search capability because there are many local minima around the global minimum as shown in Fig. 5 (c). It is very difficult to find a global minimum within the limited function in this test function. The objective of this test function is to minimize a function. This function has 220 local minima and one global minimum $f(x)=0$ at $(0,0)$.

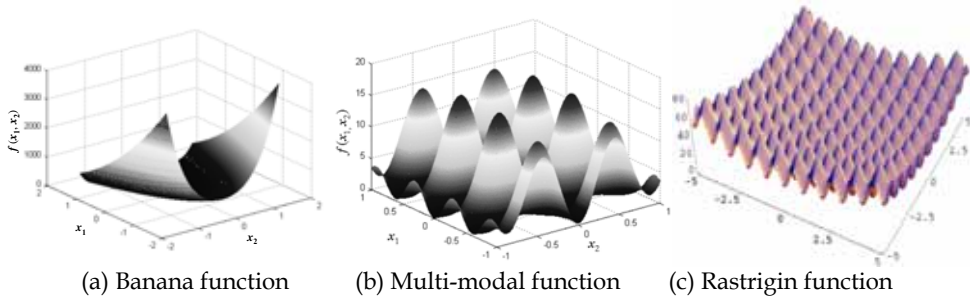


Fig. 5. Benchmark test functions

The convergence speed of the optimization algorithm is evaluated by using test function 1. The ability of searching several global minima simultaneously is evaluated by using test function 2. The global search capability among many local minima is finally evaluated by using test function 3. Table 1 shows the parameters of CHEA used in this paper.

GA	Length of chromosome	12
	Number of population	200
	Crossover probability	40%
	Mutation probability	$0.8\exp(-i_G / 2)$, i_G : ith generation
Clustering	CEF	0.2
	w_g	0.9
	w_m	1.5
	w_r	0.9
Random search	Max iteration	400

Table 1. Parameters for CHEA

To observe the searching procedure of CHEA, the gradual process of CHEA for Rastrigin function is shown in Fig. 6. GA was terminated in one cluster after six generations as shown in Fig. 6 (a). After *GA-clustering* process, local search was carried out with four randomly selected individuals from each cluster. Since the results of the local search did not converge to a point, CHEA considered this cluster to have many local minima as shown in Fig. 6 (b). Therefore, GA-clustering task was repeated with reduced search bounds. After five generations, all individuals were well clustered as shown in Fig. 6(c) where the GA was terminated. After a local search for each cluster, CHEA produced a global minimum and three local minima as shown in Fig. 6(d). No better global candidate was found during random search.

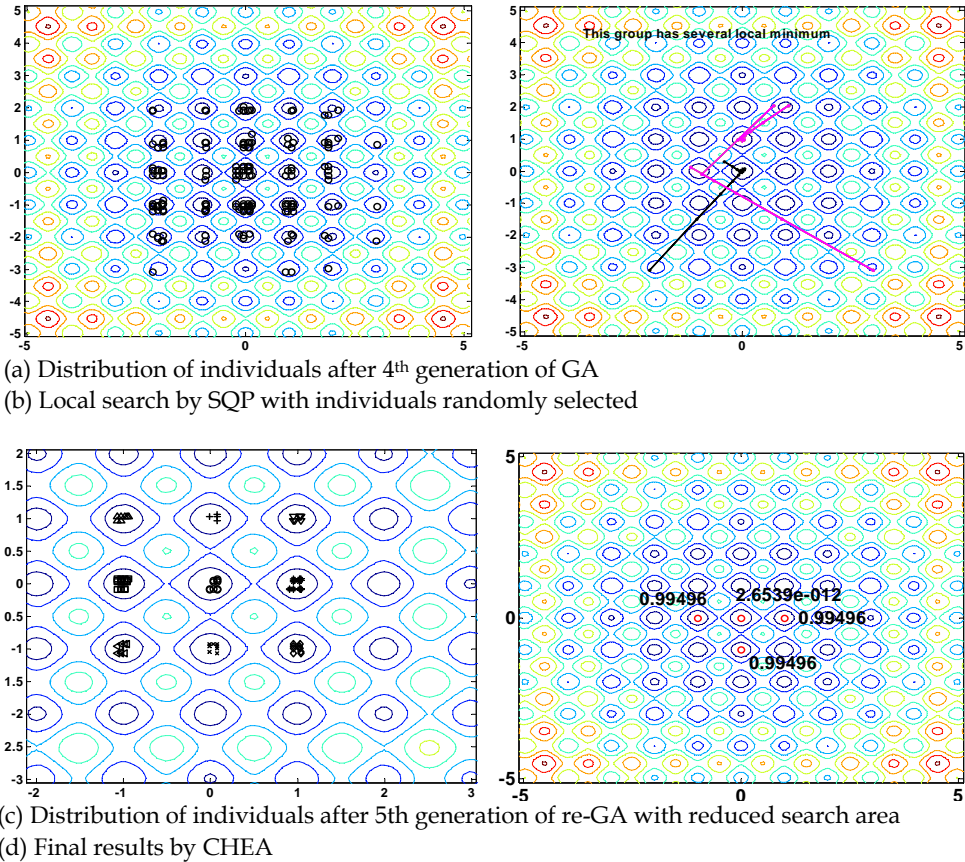


Fig. 6. Optimization procedure by CHEA for test function 3

4. Comparison of performance of CHEA

Optimization results by CHEA are compared with EGA (Kim, 2003) and ASA (Ingber & Rosen, 1992) which are known as the advanced version of GA and SA. Table 2 shows the comparison for test function 1. The second column indicates the total number of function call which also represents computation time. Third to fifth columns show the mean optimum values of the design variables and the final value of the objective function, respectively. The result using ASA did not converge well to an optimum value though it spent more computation times than those of CHEA. EGA gave the exact optimum value but took 3183 number of function calls as compared to CHEA which took 1120 functional calls. The results for test function 2 are shown in Table 3. All algorithms showed the results having similar resolution, but ASA produced only one global minimum as compared with the others which found four global minima. EGA was slower than ASA but found all the global minima. The table shows that CHEA found all global minima and with the smallest number of function call.

Finally, the test results for test function 3 are summarized in Table 4. All algorithms found the local minima, but they often failed to find the global minimum. The last column shows the percentage of success in finding the global minimum. EGA produced the worst results in terms of computation time and success ratio. CHEA although is slower than ASA but the success ratio to global minimum is more superior. Considering the convergence speed, accuracy of results and global search capability, CHEA is found to be the most efficient algorithm among the considered algorithms which are known to be efficient and fast.

	No. of function call	x_1	x_2	$f(x)$
ASA	1414	0.6995	0.4878	0.0905
EGA	3183	0.9999	1.0000	6.06e-19
CHEA	1120	1.0000	1.0000	9.94e-13

Table 2. Comparison of the results for the test function 1

	No. of function call	x_1	x_2	$f(x)$
ASA	1391	0.43881	-0.30585	16.09172
EGA	3014	-0.43880	-0.30585	16.09172
		-0.43880	-0.30585	16.09172
		-0.43880	-0.30585	16.09172
		0.43880	0.30585	16.09172
CHEA	1131	-0.43880	-0.30585	16.09172
		-0.43880	-0.30585	16.09172
		-0.43881	-0.30585	16.09172
		0.43881	0.30585	16.09172

Table 3. Comparison of the results for the test function 2

	No. of function call	x_1	x_2	$f(x)$	Success to global (%)
ASA	1336	1.82e-5	-2.55e-6	-2.55e-7	83
EGA	3131	1.00e-20	1.00e-20	3.16e-13	85
CHEA	2100	-5.72e-9	-2.81e-7	1.57e-11	99
		0.994	4.63e-8	0.994	
		-0.994	9.23e-9	0.994	
		8.69e-7	0.994	0.994	

Table 4. Comparison of the results for the test function 3

5. Unbalance response analysis of rotating shaft

In this study, the vibrations are calculated using general finite element procedures. Since the finite element discretization procedure is well documented in many literatures (Nelson, 1980; Pilkey, 1994; Choi & Yang, 2000), the details are omitted here and only the equations of motions are presented below.

5.1 Disk element

The rigid disk is modeled as a four degrees of freedom rigid body with the generalized coordinates defined as two translations V , W of the mass center in the X and Y directions and two rotations B and Γ of the plane of the disk about the X and Y axes. The rigid disk needs to be located at a finite element station. If the spin speed Ω is assumed to be constant then the coordinates \mathbf{q}^d are governed by the following equation.

$$\left(\mathbf{M}_T^d + \mathbf{M}_R^d\right) \ddot{\mathbf{q}}^d - \Omega \mathbf{G}^d \dot{\mathbf{q}}^d = \mathbf{F}^d \quad (5)$$

where \mathbf{M}_T^d , \mathbf{M}_R^d are the translational and rotational mass matrices respectively, \mathbf{G}^d is the gyroscopic matrix and \mathbf{F}^d is the force vector acting on the disk.

5.2 Shaft element

The shaft element is considered to be initially straight and modeled as an eight degrees of freedom element: two translations and two rotations at each station of the element. The cross-section of the element is taken to be circular and uniform. Continuous shaft mass with a constant density is taken as equivalent lumped mass. The inertia of each element is divided into two parts and applied at both ends of an element.

The equation of motion, in fixed frame and for a shaft element rotating with a constant speed Ω are given by,

$$\left(\mathbf{M}_T^e + \mathbf{M}_R^e\right) \ddot{\mathbf{q}}^e - \Omega \mathbf{G}^e \dot{\mathbf{q}}^e + \mathbf{K}^e \mathbf{q}^e = \mathbf{F}^e \quad (6)$$

Here \mathbf{q}^e is a (8×1) displacement vector, corresponding to the translational and rotational displacements (V , W , B , Γ) at both ends of the element. \mathbf{M}_T^e , \mathbf{M}_R^e are the translational and rotational mass matrices respectively, \mathbf{G}^e is the gyroscopic matrix, \mathbf{K}^e is the stiffness matrix and \mathbf{F}^e is the force vector acting on the shaft element.

5.3 Bearing elements

The nonlinear characteristics of the bearings can be linearized at the static equilibrium position using the assumption of a small vibration. The dynamic characteristics of the bearings are represented by eight stiffness and damping coefficients. The force acting on the shaft can be expressed as

$$\mathbf{C}^b \dot{\mathbf{q}}^b + \mathbf{K}^b \mathbf{q}^b = \mathbf{F}^b \quad (7)$$

where \mathbf{C}^b and \mathbf{K}^b are the damping and stiffness matrices of the bearing elements, respectively.

5.4 Assembly and system equation

Once equations (5) - (7) are established for a typical element, these equations are repeatedly used to generate other equations recursively for other elements. Then they are assembled to find the global equation, which describes the behavior of the entire system. The assembled damped system equation of motion in the fixed frame is of the form

$$\mathbf{M}\ddot{\mathbf{q}} + \mathbf{C}\dot{\mathbf{q}} + \mathbf{K}\mathbf{q} = \mathbf{F} \quad (8)$$

where, $\mathbf{M} = \mathbf{M}^d + \mathbf{M}^e$, $\mathbf{K} = \mathbf{K}^e + \mathbf{K}^b$, $\mathbf{C} = \mathbf{C}^b - \Omega\mathbf{G}^e - \Omega\mathbf{G}^d$. \mathbf{M} , \mathbf{C} and \mathbf{K} are total mass matrix, damping matrix and stiffness matrix, respectively. \mathbf{F} is the external force vector acting on the entire system.

5.5 Steady-state unbalance response

In fixed frame coordinates, the unbalance force in eqn. (8) is of the form

$$\mathbf{F} = \mathbf{F}_C \cos \Omega t + \mathbf{F}_S \sin \Omega t \quad (9)$$

The steady state solution is given by,

$$\mathbf{q} = \mathbf{q}_C \cos \Omega t + \mathbf{q}_S \sin \Omega t \quad (10)$$

Substituted eqns. (9) and (10) into (8) yields

$$\begin{bmatrix} \mathbf{q}_C \\ \mathbf{q}_S \end{bmatrix} = \begin{bmatrix} \mathbf{K} - \Omega^2 \mathbf{M} & -\Omega \mathbf{C} \\ \Omega \mathbf{C} & \mathbf{K} - \Omega^2 \mathbf{M} \end{bmatrix}^{-1} \begin{bmatrix} \mathbf{F}_C \\ \mathbf{F}_S \end{bmatrix} \quad (11)$$

The solution of eqn. (11) and substituting back into eqn. (10) provides the system unbalance response.

6. Optimization formulation for identification

6.1 General identification procedure

Fig. 6 shows the general identification procedure for determining the unknown system parameters, such as bearing parameters, position, magnitude and phase of unbalance of rotor-bearing system. It consists of different tasks as shown in Fig. 6. At first, a linear analytical model which is generally described by a differential equation is formulated by including unknown parameters. And then, steady-state unbalance response can be calculated by using the equations described in previous section. Such a response can also be obtained from the measurements of output signals in rotor-bearing system. Finally, in the comparison task, the analytical response is compared with the measured response at the same nodes. If their correlation is poor, the system unknown parameters are renewed and sent to the analytical model. This iterative procedure for improving the system unknown parameters is set if the correlation of model and measurement is good enough. The key issue of this procedure is how much variations of parameters have to be given to the new analytical model. It is very time consuming to do this manually. Thus many optimization techniques have been developed to solve this kind of problem which can be formulated as minimization problem.

6.2 Formulation of optimization problem

The classical nonlinear constrained optimization problem can be written mathematically as:

$$\text{Minimize } f(\mathbf{x}) \quad (12)$$

$$\text{Subject to } g_l(x) \leq 0 \ (l=1, m), \ h_k(x) = 0 \ (k = 1, n), \ x_i^l \leq x_i \leq x_i^u \ (i = 1, p) \quad (13)$$

In general, the objective function $f(\mathbf{x})$ as well as the constraint functions $g_l(\mathbf{x})$ and $h_k(\mathbf{x})$ are nonlinear implicit functions with respect to the design variables. Classical optimization algorithms require these functions to be unimodal and continuous, and their first derivatives have to be available. Otherwise, various numerical difficulties and convergence problems may arise. The global optimization algorithms, such as GA and SA, have been developed in order to overcome the above restrictions and difficulties.

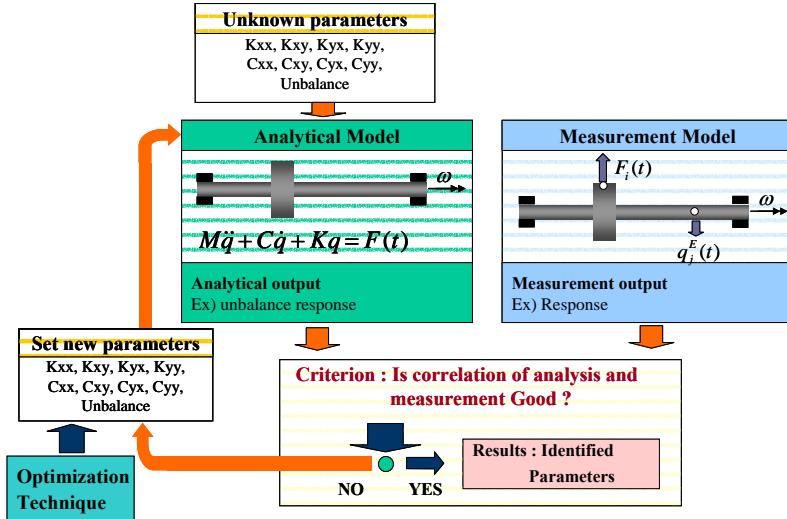


Fig. 6. General identification procedure using optimization technique

It is important to choose the form of the objective function, $f(\mathbf{x})$, in engineering application of optimization algorithms. Three different types of objective functions are considered as shown in equations (14) to (16). The sum-squared difference between the magnitude of the experimental and analytical unbalance responses, as shown in equation (14), is a common choice, but this function performs rather badly in certain practical applications, especially in low damping system. The reasons for this failure are due to the function being dominated by the contributions made at the critical speed and resonant peaks. Another possible approach is to consider the difference of the natural logarithm of the unbalance responses to reduce the weighting of the natural frequencies defined in equation (15). A simple difference function, shown in equation (16), can also be used as an objective function.

$$f_1(\mathbf{x}) = \sum_j \sum_{\Omega} (U_j^X(\Omega, \mathbf{x}) - U_j^A(\Omega, \mathbf{x}))^2 \quad (14)$$

$$f_2(\mathbf{x}) = \sum_j \sum_{\Omega} \left| \log_{10} U_j^X(\Omega, \mathbf{x}) - \log_{10} U_j^A(\Omega, \mathbf{x}) \right| \quad (15)$$

$$f_3(\mathbf{x}) = \sum_j \sum_{\Omega} \left| U_j^X(\Omega, \mathbf{x}) - U_j^A(\Omega, \mathbf{x}) \right| \quad (16)$$

where, U denotes the unbalance response and superscripts X and A represent measured and analytical responses, respectively. Ω is the rotating speed of the shaft, j is the measuring node and \mathbf{x} is the identifying parameter vector.

The optimization problem for parameters identification of rotor-bearing system is formulated as follows:

Minimize $f(\mathbf{x})$

$$\text{subject to: } x_i^l \leq x_i \leq x_i^u, \quad x_i \in \mathbf{x}, \quad x_i = 1, 2, \dots, 5 \quad (17)$$

and the design variables: $\mathbf{x} = (k_{xx}, k_{xy}, k_{yx}, k_{yy}, c_{xx}, c_{xy}, c_{yx}, c_{yy}, u)$

where, x_i is the design variable and superscripts l and u represent the lower and upper bounds of the design variables, respectively. k_{ij}, c_{ij} ($i, j = x, y$) are the stiffness coefficients and damping coefficients of bearing respectively. Subscript x and y denote horizontal and vertical direction, respectively. u denotes the residual unbalance of the disk.

In this study, only the diagonal terms of the stiffness and damping coefficients ($k_{xx}, k_{yy}, c_{xx}, c_{yy}$) are considered and does not consider inequality or equality constraints. When a journal bearing is used in the rotor-bearing system, cross-coupled terms of stiffness and damping coefficients ($k_{xy}, k_{yx}, c_{xy}, c_{yx}$) need to be selected as design variables.

7. Numerical application

The proposed methodology is first verified by a simulation study. A simple rotor-bearing model is shown in Fig. 7 and detail specifications of the rotor bearing model are shown in Table 5. The rotor system consists of a shaft of 1.3m in length and 0.1m in diameter, and has three disks. Two bearings support the shaft at the each ends. The dynamic coefficients of the two bearings are of the same values, and hence only the diagonal terms are considered. An unbalance mass was added on disk 2 (6th node) with a magnitude of 200 g·mm and an angle of 0° . The unbalance responses at the 2nd and the 12th nodes were selected as simulated measured responses. To consider the uncertainty of the analytical model and to examine the robustness of identification, 10% of Gaussian noise was applied to the simulated responses.

The stiffness and damping coefficients of the bearing and the magnitude of unbalance mass on disk were chosen as identifying parameters. The formulation of optimization is described in the following section.

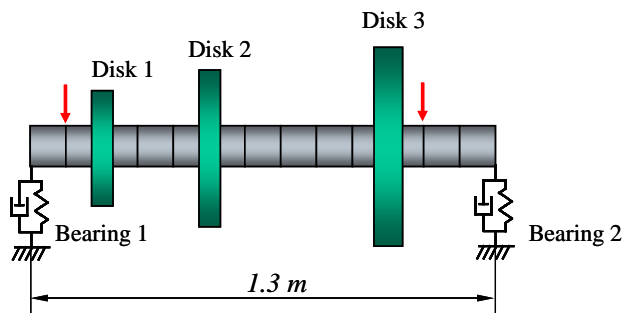


Fig. 7. Rotor bearing model (Lalanne and Ferraris, 1998)

Shaft	Shaft length (m)	1.3
	Shaft diameter (m)	0.1
	Young's modulus (GPa)	200
	Density (kg/m ³)	7,800
	Poisson ratio	0.3
Bearing	k_{xx}, k_{yy} (MN/m)	50, 70
	c_{xx}, c_{yy} (kN·s/m)	0.5, 0.7
	$k_{xy}, k_{yx}, c_{xy}, c_{yx}$	0

Table 5. Model parameters in Lalanne's rotor model

7.1 Formulation of optimization

Objective function

$$f_1(\mathbf{x}) = \sum_{j=v,h} \sum_{\Omega} (U_j^X(\Omega, \mathbf{x}) - U_j^A(\Omega, \mathbf{x}))^2$$

$$\text{Minimize } f_2(\mathbf{x}) = \sum_{j=v,h} \sum_{\Omega} |\log_{10} U_j^X(\Omega, \mathbf{x}) - \log_{10} U_j^A(\Omega, \mathbf{x})| \quad (18)$$

$$f_3(\mathbf{x}) = \sum_{j=v,h} \sum_{\Omega} |U_j^X(\Omega, \mathbf{x}) - U_j^A(\Omega, \mathbf{x})|$$

where, U_j is vertical and horizontal responses at 2nd and 12th nodes, respectively and Ω is rotating speed ranging from 200 to 15000 rpm with a step of 200 rpm.

Design variables (Identifying parameters)

$$\mathbf{x} = (k_{xx}, k_{yy}, c_{xx}, c_{yy}, u) \quad (19)$$

where, k_{xx} and k_{yy} are the horizontal and vertical stiffness coefficients, c_{xx} and c_{yy} are the horizontal and vertical damping coefficients, respectively. u is the magnitude of mass unbalance of disk.

Side constraints

$$10^2 \leq k_{xx}, k_{yy} \leq 10^9 \text{ (N/m)}, 10^0 \leq c_{xx}, c_{yy} \leq 10^7 \text{ (N·s/m)}, 10^{-7} \leq u \leq 10^{-2} \text{ (kg·m)} \quad (20)$$

The control parameters for this algorithm are listed in Table 6. These parameters are determined by considering the global search capability and the computation time.

GA	Length of chromosome	12
	Number of population	200
	Crossover probability	40%
	Mutation probability	$0.8 \exp(-i_G / 2)$, i_G : i th generation
Clustering	CEF	0.2
	w_g	0.9
	w_m	1.5
	w_r	0.9
Random search	Max iteration	500

Table 6. Control parameters for optimization algorithm (CHEA)

7.2 Identification results

Table 7 shows the identification results using the simulated unbalance response without noise. With the objective functions of all cases, all identified parameters have exactly the same reference values and the total call number of the objective function is about 3000. Fig. 8 shows the history of the objective function values. It can be seen that, after 6th generation, GA-clustering task was terminated and yielding the classification to one cluster. In a local search, three points converged to one point and consumed 1300 times of function evaluations. With a total of 500 trials of random searches the algorithms were unable to locate the lower local minimum candidate and the program had to be terminated. The result clearly shows that the shape of objective function needs to be a wide concave type.

Design variables	Reference values	Identified values		
		$f_1(\mathbf{x})$	$f_2(\mathbf{x})$	$f_3(\mathbf{x})$
k_{xx} (MN/m)	50	50	50	50
k_{yy} (MN/m)	70	70	70	70
c_{xx} (kN·s/m)	0.5	0.5	0.5	0.5
c_{yy} (kN·s/m)	0.7	0.7	0.7	0.7
u (g·mm)	200	200	200	200
No. of function call		2,993	2,768	3,150

Table 7. Identification results using the unbalance response without noise

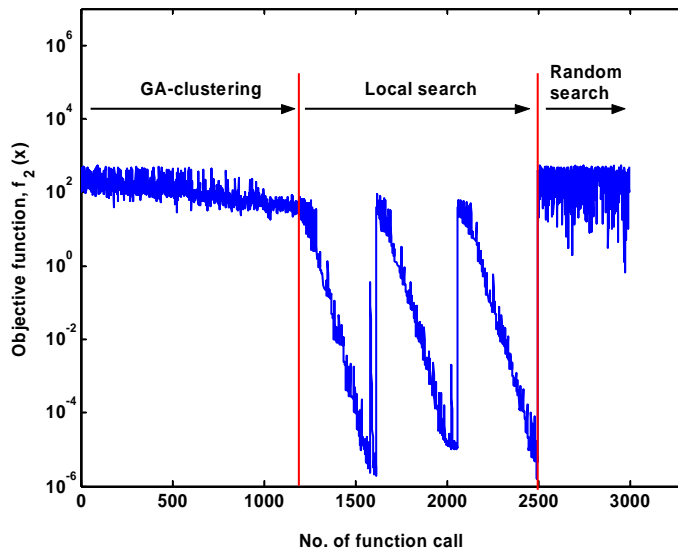


Fig. 8. History of objective function values

The identification results using a simulated response with 10% Gaussian noise added are summarized in Table 8, taking into consideration the three kinds of objective functions. In the case of function $f_1(\mathbf{x})$, the errors of stiffness coefficients varied from 2.4% to 8.1% and are less than 10%. However, the errors due to damping coefficients fluctuate significantly. The

results by using function $f_3(\mathbf{x})$ are not acceptable due to the high errors encountered in stiffness coefficients, ranging from 14.8% to 160%. In the case of function $f_2(\mathbf{x})$, which is considered to be the best choice, the stiffness coefficients and magnitude of mass unbalance (u) are well identified with error less than 1% with respect to the reference values. This is obtained by excluding the relative higher errors of damping coefficients. The reasons for the poor results with respect to the damping coefficients are

- The damping coefficients of the bearing strongly affect the magnitude of the unbalance response near the resonant peaks in a low damping system.
- The peak value of the response fluctuates to the higher values than other responses due to the Gaussian noise.

Design variables	Reference value	Objective function (% error)		
		$f_1(\mathbf{x})$	$f_2(\mathbf{x})$	$f_3(\mathbf{x})$
k_{xx} (MN/m)	50	45.94 (8.1)	50.16 (0.3)	112.1 (124)
k_{yy} (MN/m)	70	71.67 (2.4)	69.94 (0.1)	80.38 (14.8)
c_{xx} (kN·s/m)	0.5	2.570 (414)	0.434 (13.8)	0.852 (160)
c_{yy} (kN·s/m)	0.7	0.0015 (99)	0.684 (4.1)	0.834 (19)
u (g·mm)	200	210.4 (5.2)	200.8 (0.3)	115.8 (42)

Table 8. Comparison of identification results for different objective functions in the case 10% Gaussian noise added to unbalance response

From these results, the objective function needs to be selected carefully by considering the shape of the measured response function. Fig. 9 shows the simulated unbalance responses with 10% Gaussian noise added and the calculated unbalance responses using the identified parameters for the case function $f_2(\mathbf{x})$. The identified response is in good agreement with the simulated measured ones.

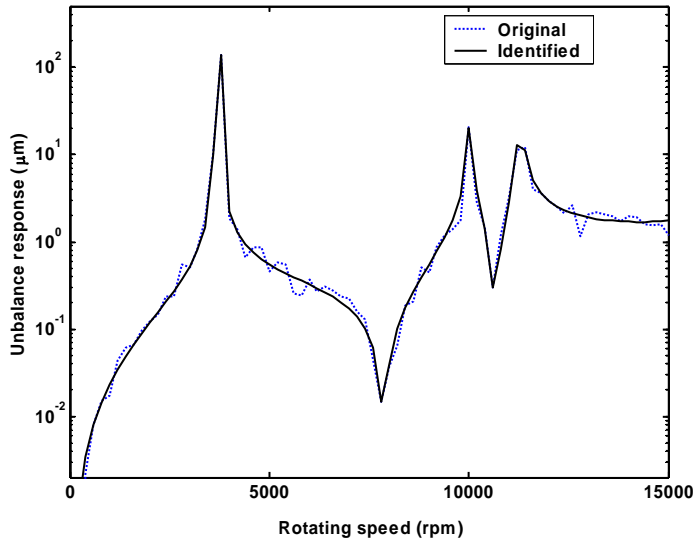


Fig. 9. Original and identified unbalance response

8. Experimental validation

The experimental validation was performed to verify the effectiveness of proposed identification approach. By using a Rotor-Kit system, the stiffness coefficients and unbalance mass of disk are identified simultaneously. The identified results are compared with those obtained by measurement.

8.1 Test rig and measured response

The test rig for experimental validation is shown in Fig. 10. The rotor-system is the RK4 model manufactured by Bently-Nevada. A flexible coupling connects a controllable DC motor to the shaft. Spring-bearing, which has four springs for driving a ball bearing in all directions as shown in Fig. 10, was used to identify the stiffness and damping coefficients. The adjoined two ball bearings in the coupling side are used to prevent slight angular movements which usually occurred in single ball bearing setup. Two proximity probes are incorporated to measure the shaft vibration in the vertical and horizontal directions.



Fig. 10. Experimental test rig

Fig. 11 shows the schematic of the test setup with the spring-bearing. The measured signal was processed by using the DAI-108 and ADRE software. The stiffness of the two adjoined ball bearings in the left side was considered to be rigid because it was significantly greater than the identifying stiffness of the spring-bearing at the right side. The parameters of the shaft, disk and spring-bearing are listed in Table 9. To identify the unknown parameters in a real system, all the other parameters need to be defined. Therefore, Young's modulus and density of shaft listed in Table 5 were updated by using the model updating technique.

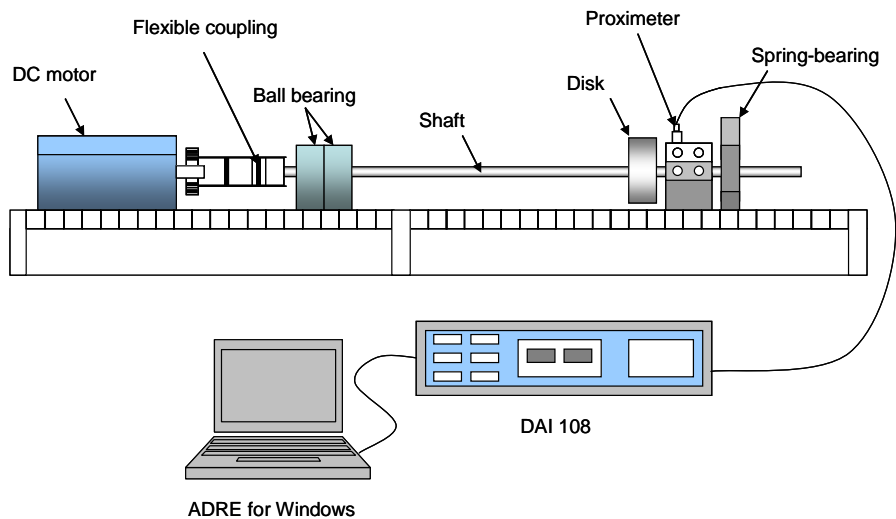


Fig. 11. Schematic of an experimental setup with a spring-bearing

Shaft	Length (mm)	560
	Diameter (mm)	10
	Density (kg/m ³)	7,801
	Young's modulus (MPa)	208.11
	Poisson ratio	0.3
Disk	Mass (kg)	0.809
	Polar moment of inertia (kg m ²)	568.46×10^{-6}
	Trans. moment of inertia (kg m ²)	327.60×10^{-6}
	Magnitude of unbalance (g mm)	15
Bearing	Bearing span (mm)	401
	Horizontal stiffness (kN/m)	33.9
	Vertical stiffness (kN/m)	33.6

Table 9. Parameters of test setup

Fig. 12 shows a 1X filtered measured response of horizontal vibration according to speed-up and speed-down of the motor. Slow roll vector at 500 rpm was used to compensate the original signal. The response below the critical speed was used in the identification process because they increased sharply near the critical speed. In actual fact, many rotating systems operate below the first critical speed. The reason why the measured signal is not smooth enough is because this system has no damping mechanism except internal material damping or friction. Fig. 13 shows, for example, an instantaneous measured signal in the vertical direction at a shaft speed of 1350 rpm. The first peak in the spectrum plot indicates the rotating speed and the second peak is the first natural frequency of the system. This appearance is frequently shown in low damping systems supported by ball bearings. Furthermore, traditional deterministic identification approaches (Lee & Hong, 1988; Chen & Lee, 1995, 1997; Tiwari et al., 2002) often failed to identify the exact parameters.

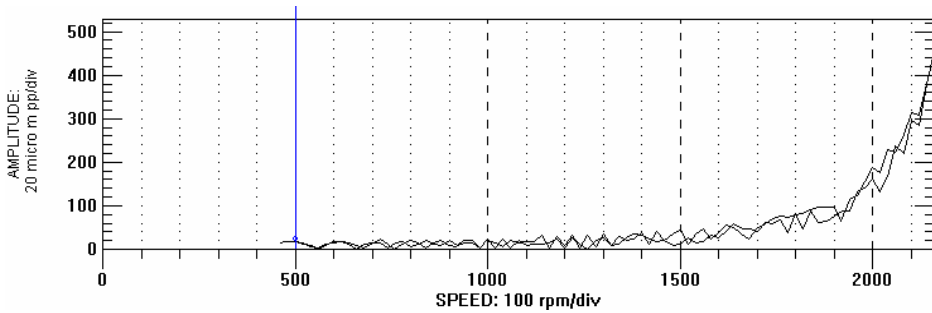


Fig. 12. 1X filtered measured horizontal response

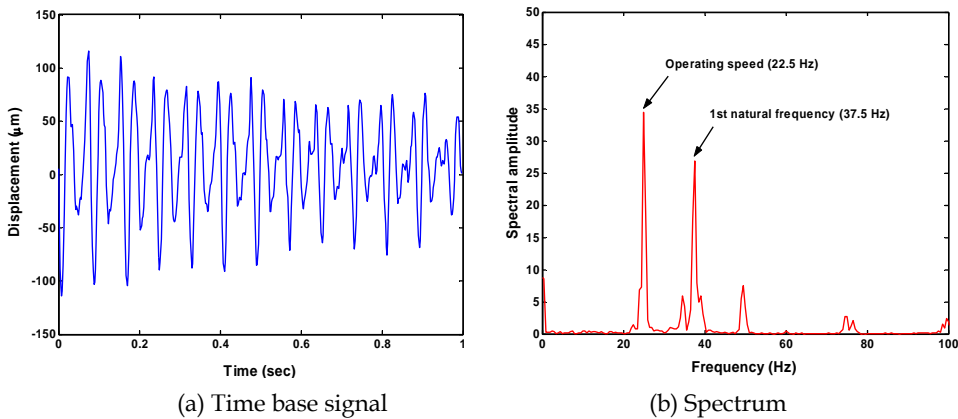


Fig. 13 Instantaneous vibration signal and its spectrum at 1350 rpm

8.2 Optimization formulation and results

The same control parameters for optimization algorithm listed in Table 2 are used in this case. By using the above measured responses in the vertical and horizontal directions, optimization for identifying the bearing parameters and unbalance is formulated as follows:

Objective function:

$$f_1(\mathbf{x}) = \sum_j \sum_{\Omega} (U_j^X(\Omega, \mathbf{x}) - U_j^A(\Omega, \mathbf{x}))^2$$

$$\text{Minimize } f_2(\mathbf{x}) = \sum_j \sum_{\Omega} |\log_{10} U_j^X(\Omega, \mathbf{x}) - \log_{10} U_j^A(\Omega, \mathbf{x})| \quad (20)$$

$$f_3(\mathbf{x}) = \sum_j \sum_{\Omega} |U_j^X(\Omega, \mathbf{x}) - U_j^A(\Omega, \mathbf{x})|$$

where, U_j is response at the position of sensors and Ω is the rotating speed from 480 to 2140 rpm with a step of 20 rpm.

Design variables (Identifying parameters):

$$\mathbf{x} = (k_{xx}, k_{yy}, c_{xx}, c_{yy}, u) \tag{21}$$

where, k_{xx} and k_{yy} are the horizontal and vertical stiffness coefficients, c_{xx} and c_{yy} are the horizontal and vertical damping coefficients, respectively. u is the magnitude of mass unbalance of disk.

Side constraints:

$$10^2 \leq k_{xx}, k_{yy} \leq 10^6 \text{ (N/m)}, 10^0 \leq c_{xx}, c_{yy} \leq 10^3 \text{ (N}\cdot\text{s/m)}, 10^{-7} \leq u \leq 10^{-3} \text{ (kg}\cdot\text{m)}$$

The identification results for the spring-bearing system are summarized in Table 10. The results show an average function call number of 4327 which corresponds to a computation CPU time of 3519 second on the P-IV 3.0 GHz PC. The reference values for the stiffness coefficients were obtained from static deflection tests. The percent error of identified parameters to reference values is given in terms of percentage error (% error).

Design variables	Experimental value	Identified values (% error)		
		$f_1(\mathbf{x})$	$f_2(\mathbf{x})$	$f_3(\mathbf{x})$
k_{xx} (kN/m)	33.900	30.884 (8.9)	30.796 (9.1)	33.491 (1.2)
k_{yy} (kN/m)	34.600	34.203 (1.1)	34.001 (1.7)	36.390 (5.2)
c_{xx} (N·s/m)	–	13.42	11.96	15.44
c_{yy} (N·s/m)	–	16.06	14.11	3.16
u (g mm)	15	13.82 (7.8)	12.86 (14.3)	16.13 (7.5)
No. of total function call		4,334	4,360	4,288

Table 10. Identification results for the spring-bearing system

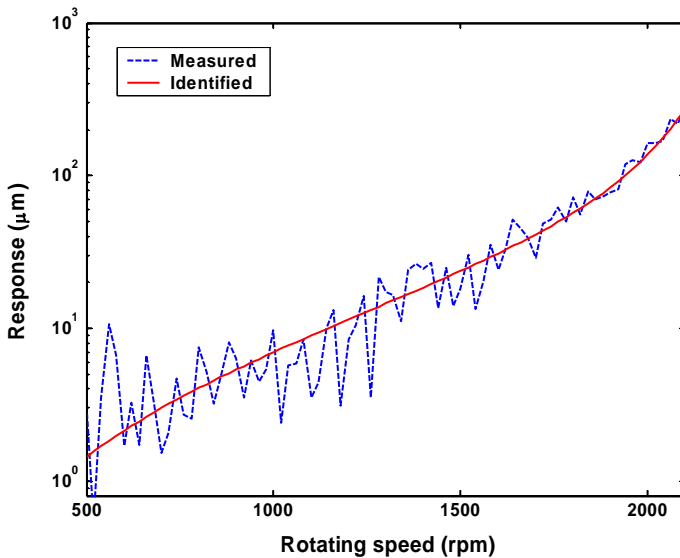


Fig. 14. Measured and Identified horizontal unbalance response for $f_3(\mathbf{x})$

Although the 1X amplitude of the measured signal had significant fluctuation, all the identified parameters fitted well with the reference values. Considering the percentage error to reference values, as shown in the Table 10, the best choice of the objective function is $f_3(\mathbf{x})$, which is the sum of differences between measured and analytical responses. Fig. 14 shows the identified horizontal unbalance response and 1X filtered measured response at the sensor positions. From this result, it is verified that the proposed methodology could be effectively used to identify bearing coefficients with the magnitude of unbalance using the measured unbalance responses.

9. Conclusions

A new hybrid evolutionary algorithm using clustering-based hybrid evolutionary algorithm (CHEA), is proposed in this chapter. The main feature of CHEA is the clustering of individuals introduced for evaluating the degree of maturity of genetic evolution. After the clustering-based genetic algorithm, local search is carried for each cluster in this algorithm. CHEA attempts to find each local minimum from each cluster or continues with GA focusing on the regions of each cluster until all significant local minima are found. Therefore CHEA can lead to local minima as well as global minimum. ART-Kohonen neural network (ART-KNN) is used in the clustering of individuals in GA. Sequential quadratic programming (SQP) is adopted as local search. An efficient random search is introduced for improving the probability of finding the global minimum which may be missed by GA or local search task. The effectiveness of the proposed algorithm was evaluated using three well-known benchmark functions. The results showed that the CHEA reached the global minimum faster than EGA and ASA. It has the ability to find the global minimum as well as the local minima and having higher global search capability than other algorithms.

When using CHEA for parameter identification of bearings, it optimizes the formulation process to achieve an optimum solution. It minimizes the differences between analytical unbalance responses and measured ones by considering the unknown bearing parameters as design variables. Three types of feasible objective functions were applied in evaluation process, namely, sum-squared differences, logarithmic differences and simple differences to find the most competent formulation of the objective function. The magnitude of mass unbalance was also chosen as identifying parameters. Numerical and experimental applications were presented to confirm the effectiveness of this methodology. In the numerical application, 10% of Gaussian noise was added to simulate measured response and to examine the robustness of the methodology. The results showed that the unknown parameters were correctly identified and the logarithmic differences function was concluded as the best objective function in the numerical simulation. When applied to an experimental rotor-bearing system the measured synchronous response fluctuates according to the rotating speeds but the identified parameters fitted well with the reference values. This new algorithm has the potential for use in real life applications. However, further investigations using industrial data are required to test the robustness of the technique before applying the method to industrial rotating machinery.

10. Acknowledgement

The work is partially supported by the CRC for Integrated Engineering Asset Management (CIEAM), Australia.

11. References

- Berger, J., Sassi, M. and Salois, M. (1999) A hybrid genetic algorithm for the vehicle routing problem with time windows and itinerary constraints, in Proceedings of the Genetic and Evolutionary Computation Conference, Orlando, USA, pp. 44–51
- Burrows, C. R. & Stanway, R. (1977) Identification of journal bearing characteristics. ASME J Dynamic System Measurement and Control, Vol. 99, pp. 167-175
- Carpenter GA, Grossberg S (1988) The art of adaptive pattern recognition by a self-organizing neural network. IEEE Trans on Computer, Vol 21, No. 3, pp. 77-88
- Chen, J. H. & Lee, A. C. (1995) Estimation of linearized dynamic characteristics of bearings using synchronous response. International Journal of Mechanical Science, Vol. 37, No.2, pp. 197-219
- Chen, J. H. & Lee, A. C. (1997) Identification of linearised dynamic coefficients of rolling element bearings. ASME Journal of Vibration and Acoustics, Vol. 119, pp. 60-69
- Choi, B. G. & Yang, B. S. (2000) Optimum shape design of shaft using genetic algorithm. J of Vib and Control 6(1): 207- 220
- Edwards, S.; Lees, A. W. & Friswell, M. I. (2000) Experimental identification of excitation and support parameters of a flexible rotor- bearings-foundation system from a single run-down. Journal of Sound and Vibration, Vol. 232, No. 5, pp. 963-992
- Fletcher, R. (1980) Practical methods of optimization, Constrained Optimization. John Wiley and Sons
- Fung, R. Y. K., Tang, J. and Wang, D. (2002) Extension of a hybrid genetic algorithm for nonlinear programming problems with equality and inequality constrains, Computers & Operations Research, Vol. 29, No. 3, pp. 261–274
- Hageman, J. A., Wehrens, R., Sprang, H. A. and Buydens, L. M. C. (2003) Hybrid genetic algorithm-tabu search approach for optimizing multilayer optical coatings, Analytica Chimica Acta, Vol. 490, pp. 211–222
- He, D., Li, Y. and Wang, F. (2001) Hybrid genetic algorithm based on the operator of pattern search, Information and Control, Vol. 30, No. 3, pp. 276–278
- Hsiao, C. T., Chahine, G. and Gumerov, N. (2001) Application of a hybrid genetic algorithm/Powell algorithm and a boundary element method to electrical impedance topography, Journal of Computational Physics, 173, 433-454
- Ingber, L. and Rosen, B. (1992) Genetic algorithms and very fast simulated re-annealing: a comparison, Mathematic Computational Modeling, Vol. 16, pp. 87–100
- Jiang, Z., Liu, B., Dai, L. and Wu, T. (2003) A hybrid genetic algorithm integrated with sequential linear programming, in Proceedings of the Second International Conference on Machine Learning and Cybernetics, Xian, pp. 1030–1033
- Kim, Y. C. (2003) Development of Enhanced Genetic Algorithm and Its Applications to Optimum Design of Rotating Machinery, Ph.D. Dissertation, Pukyong National University, South Korea
- Kim, Y. H., Yang, B. S. and Tan, A. C. C. (2006) Clustering-based Hybrid Evolutionary Algorithm for Optimization, Advances in vibration engineering, Vol. 5, No. 2, pp. 163-173
- Kim, Y. H., Yang, B. S. and Tan, A. C. C. (2007) Bearing Parameter Identification of Rotor-Bearing System Using Clustering-based Hybrid Evolutionary Algorithm, Structural and Multidisciplinary Optimization, Vol. 33, No. 6, pp. 493-506
- Kirpatrick, S. C. D. & Gelatt, M. P. (1983) Optimization by simulated annealing. Science Vol. 220, No. 4598, pp. 671–680

- Kohonen, T. (1995) *Self-Organizing Maps*, New York: Springer-Verlag
- Kraus, J.; Blech, J. J. & Braun, S. G. (1987) In situ determination of rolling bearing stiffness and damping by modal analysis. *ASME J Vibration, Acoustics, Stress, and Reliability in Design*, Vol. 109, pp. 235-240
- Lee, C. W. & Hong, S. W. (1988) Identification of bearing dynamic coefficients by unbalance response measurements. *Proceedings of Institution of Mechanical Engineers Vol. 203C*, pp. 93-101
- Lee, C. Y., Gen, M. and Kuo, W. (2001) Reliability optimization design using hybridized genetic algorithm with a neural network technique, *IEICE Trans. on Fundamental*, Vol. E84-A, No. 2, pp. 627–637
- Liu, Y., Ma, L. and Zhang, J. (2002) Reactive power optimization by GA/SA/TS combined algorithms, *Electrical Power and Energy Systems*, Vol. 24, pp. 765–769, 2002
- Nelson, H. D. (1980) A finite rotating shaft element using Timoshenko beam theory. *ASME, J Mechanical Design* 102: 793-803
- Ong, S. K., Ding, J. and Nee, A. Y. C. (2002) Hybrid GA and SA dynamic set-up planning optimization, *International Journal of Production Research*, Vol. 40, No. 18, pp. 4697–4719
- Pilkey, W. D. (1994) *Formulus for stress, strain, and structural matrices*. John Wiley, New York, USA
- Ponnambalam, S. G. and Reddy, M. M. (2003) A GA-SA multiobjective hybrid search algorithm for integrating lot sizing and sequencing in flow-line scheduling, *International Journal of Advanced Manufacturing Technology*, Vol. 21, pp. 126–137
- Powell, M. J. D. (1978) A fast algorithm for nonlinearly constrained optimization calculations. *Numerical Analysis*, G.A.Watson ed., *Lecture Notes in Mathematics*, Springer Verlag, 630
- Reddy, V. B.; Tiwari, R. & Kakoty, S. K. (2002) Identification of bearing dynamic parameters from impulse response of rotor bearing systems. *Proceedings of VETOMAC-2*
- Renders, J. M. and Flasse, S. P. (1996) Hybrid methods using genetic algorithms for global optimization, *IEEE Transactions on Systems, Man, and Cybernetics Part B*, Vol. 26, No. 2, pp. 243–258
- Roach, A. and Nagi, R. (1996) A hybrid GA-SA algorithm for just-in-time scheduling of multi-level assemblies, *Computers Industrial Engineering*, Vol. 30, No. 4, pp. 1047–1060
- Schittkowski, K. (1985) NLQPL: A FORTRAN-subroutine solving constrained nonlinear programming problems. *Annals of Operations Research* 5: 485-500
- Tiwari, R.; Lees, A. W. & Friswell, M. I. (2002) Identification of speed-dependent bearing parameters. *Journal of Sound and Vibration*, Vol. 254, No. 5, pp. 967-986
- Wu, Z., Shao, H. and Wu, X. (1999) A new adaptive genetic algorithm & its application in multimodal function optimization, *Control Theory and Applications*, Vol. 16, No. 1, pp. 127–129
- Yang, B. S.; Han, T. & An, J. L. (2004) ART-Kohonen neural network for fault diagnosis of rotating machinery. *Mechanical System and Signal Processing*, Vol. 18, pp. 645-657
- Yu, H., Fang, H., Yao, P. and Yuan, Y. (2000) A combined genetic algorithm/simulated annealing algorithm for large scale system energy integration, *Computers and Chemical Engineering*, Vol. 24, pp. 2023–2035